energies

MDPI

Article

Effects of Oxygen-Enhanced Combustion Methods on Combustion Characteristics of Non-Premixed Swirling Flames †

Pavel Skryja [1], Igor Hudak [1], Jiří Bojanovsky [1], Zdeněk Jegla [1,*] and Lubomír Korček [2]

[1] Institute of Process Engineering, Faculty of Mechanical Engineering, Brno University of Technology, Technická 2, 616 69 Brno, Czech Republic; skryja@fme.vutbr.cz (P.S.); igor.hudak@vutbr.cz (I.H.); jiri.bojanovsky@vutbr.cz (J.B.)
[2] UNIS, a.s., Jundrovská 33, 624 00 Brno, Czech Republic; korcek@unis.cz
* Correspondence: zdenek.jegla@vut.cz
† This paper is an extended version of our paper published in 2014, Experimental study on the influence of oxygen content in the combustion air on the combustion characteristics, Energy, October 2014, Volume 75, Pages 116–126.

Abstract: The objective of the present study was to experimentally investigate and compare the characteristics of three oxygen-enhanced combustion (OEC) methods; premix enrichment (PE), air-oxy/fuel combustion (AO), and additionally also oxygen lancing (OL) method. The overall oxygen concentration varied from 21% to 38%. Combustion tests were carried out using the gas burner with the thermal input of 750 kW fired by natural gas. The characteristics of OEC methods, such as the concentration of nitrogen oxides and carbon monoxide in flue gas, in-flame temperatures distribution in the horizontal symmetry plane of the combustion chamber, heat flux to the combustion chamber wall, flue gas temperature, and the stability of flame were investigated. NO_x emissions increased by more than 40 times and by 20 times for the PE method. The tests using the AO and OL methods with NO_x emissions below 150 mg/Nm^3 at all oxygen concentrations showed significantly better results. For all OEC methods, radiative heat transfer increased with increasing oxygen concentration. The available heat was 20% higher at 38% O_2 than at 21% O_2. The flue gas temperature decreased with increasing oxygen concentration, which was affected by a decrease in N_2 concentration in the oxidizer and a simultaneous increase in radiant heat flux.

Keywords: oxygen-enhanced combustion; nitrogen oxides; heat flux; in-flame temperature; flame stability; oxygen lancing method

Citation: Skryja, P.; Hudak, I.; Bojanovsky, J.; Jegla, Z.; Korček, L. Effects of Oxygen-Enhanced Combustion Methods on Combustion Characteristics of Non-Premixed Swirling Flames. *Energies* **2022**, *15*, 2292. https://doi.org/10.3390/en15062292

Academic Editor: Michael Liberman

Received: 22 February 2022
Accepted: 17 March 2022
Published: 21 March 2022

1. Introduction

Most industrial high-temperature heating processes, such as incineration, ferrous and nonferrous metal smelting, and glass and cement melting require a considerable supply of heat commonly available from fossil fuels combustion [1]. Most industrial combustion processes use the atmospheric air as the oxidant, consisting of ca. 21% O_2 and 79% N_2 by volume. However, it is only oxygen that is needed in the reactions with hydrocarbons, while nitrogen is the inert gas that must be heated up and carries a part of the energy of the combustion away with the hot flue gases. This lowers the heat transfer efficiency of the combustion process. In contrast, the oxygen-enhanced combustion (OEC) [2] can eliminate this drawback because the oxygen concentration is higher than that in the ambient air. It is evident that OEC methods provide several benefits to the operation of industrial furnaces, such as increased processing rates, higher heat transfer efficiency, higher turndown of the burners, enhanced flame stability, reduced equipment cost, and better product quality [2].

Additionally, the lower nitrogen concentration in the air reduces flue gas flow rates and, thus, the energy losses to the ambient. The use of OECs leads to an increased radiation flux in the combustion chamber and may damage the refractory lining of the furnace or burners. Higher NO_x production must also be considered.

Combustion processes can be enhanced by four OEC methods [2]: (1) adding O_2 into the incoming airstream (referred to as the premix enrichment), (2) injecting O_2 into an air/fuel flame (referred to as the oxygen lancing), (3) separately provided combustion air and O_2 to the burner (referred to as the air-oxy/fuel combustion), (4) replacing the combustion air with high-purity O_2 (referred to as the oxy/fuel combustion) that is known as a promising technology for capturing of CO_2 because of its high partial pressure from the flue gas [3–6].

From an economic perspective, the OEC methods (1)–(3) can save the cost for retrofits of existing burners and combustion equipment when the process is designed to operate at slightly higher oxygen concentrations. This is primarily used when the expected production rate of heating processes should be significantly increased with a relatively small oxygen enrichment. However, detailed characteristics of the OEC methods applied in the air/gaseous fuel combustion systems have not been sufficiently reported so far. Wu et al. [7] studied the influence of 21–30% oxygen concentration on the heating rate, emissions, temperature distributions, and fuel consumption in the heating and furnace-temperature fixing tests. As for the heating rate, the time required for heating to 1200 °C was only 46% for the air with 30% O_2 compared to the air with 21% O_2. NO_x emissions were increased by 4.4 times, and CO_2 increased almost linearly when the oxygen concentration increased from 21% to 30%. The furnace-temperature fixing tests showed that the fuel consumption at 30% O_2 was reduced by 26% compared with the fuel consumption at 21% O_2.

The effect of the oxygen enrichment on the stability of methane–air non-premixed swirling flame and pollutant emissions, such as CO, CO_2, and NO_x, was studied by Merlo et al. [8]. The authors reported that oxygen enrichment promotes higher CO conversion into CO_2. NO_x emissions increase significantly with oxygen addition mainly due to the increase in flame temperature. The flame stability is enhanced with oxygen enrichment, even for low oxygen enrichment rates. Tan et al. [9] used a down-fired vertical combustor to study the oxygen-enhanced and O_2/CO_2 combustion. The authors concluded that very high NO_x emissions are achieved due to higher flame temperatures related to a higher oxygen concentration in the feed air for the oxygen-enhanced combustion. However, in the O_2/CO_2 atmosphere, the NO_x formation is suppressed because N_2 is not present in the feed air; only the air leakage at the fan contributed to the NO_x formation in small concentrations. In large steam boilers, the use of OEC leads to the increase in the flue gas temperature; therefore, the heat transfer surfaces can be reduced due to the higher mean log temperature differences within the heat exchangers of the boiler. Simultaneously, the boiler's efficiency can be increased by 2% up to 5% [10]. Sánchez et al. [11] investigated the effect of oxygen enrichment from 21% to 35% by volume on the performance of a flameless combustion furnace equipped with a regenerative burner. The results showed that it was possible to obtain no luminous effect, wide reaction zone, and uniform temperature profile for all oxygen enrichment rates, which are typical features of flameless combustion phenomena. NO_x emissions were below 5 ppm, and the global efficiency increased almost by 5% for an oxygen-enriched level of 30%.

Studies [12–14] investigated the membrane separation as an air-enrichment technique. Qiu and Hayden [12] explored the OEC of natural gas in porous ceramic radiant burners where the oxygen-enriched air was produced passively using polymer membranes. The oxygen concentration varied between 21% and 28%. The experimental results showed that the potential saving in natural gas consumption was ca. 22%, with the oxygen concentration increasing to 28%.

The present paper is an extension of the study by Bělohradský et al. [15] focused on the investigation of two oxygen-enhanced combustion methods: the premix enrichment (PE) and the air-oxy/fuel combustion (AO). The major focus of our follow-up study was the experimental investigation of the third OEC method—oxygen lancing (OL), the measurement of in-flame temperatures distribution in the horizontal symmetry plane of the combustion chamber, and the overall comparison of the characteristics of all three OEC methods. The combustion tests were conducted using the specialty experimental

two-staged gas burner at the burner testing facility with the burner power of 750 kW for one-staged or two-staged combustion regimes. The desired oxygen concentration in the dry flue gas was close to 3% by volume during all measurements. However, the overall oxygen concentration in the oxidant varied from 21% to 38%, which corresponds to the additional flow rate of high-purity oxygen in the range from 0 to 100 Nm^3/h ("N" stands for the normal conditions, i.e., t = 0 °C, p = 101.325 kPa). In addition, the characteristics of OEC methods were investigated (concentration of NO_x and CO emissions in flue gas, flue gas temperature, in-flame temperatures distribution in the horizontal symmetry plane of the combustion chamber, and the stability of flame).

2. Experimental Setup

2.1. Burner Testing Facility

Combustion tests were carried out at the large-scale burner testing facility (Figure 1). The facility enables testing of gaseous fuel burners, liquid fuel burners, and/or dual fuel burners up to the thermal input of 1800 kW. A detailed description of the testing facility can be found in [15,16]. A simplified block diagram of the burner testing facility is shown in Figure 2.

Figure 1. The burners testing facility.

The crucial apparatus of the facility is a two-shell horizontal water-cooled combustion chamber with an inner diameter of 1 m and a length of 4 m. The chamber's front and rear sides are insulated using the high-temperature fibrous lining with a thickness of 100 mm. The cooling shell of the combustion chamber is divided into seven individual sections with an independent supply of cooling water. Six sections are 0.5 m long while the seventh section is 1 m long. Each section is equipped with sensors to measure the flow rate, inlet, and outlet temperature of cooling water. Thus, this unique construction enables the partial simulation of the conditions similar to those in fired process heaters and the heat flux rate from the hot flue gas to the combustion chamber shell lengthwise the flame to be evaluated.

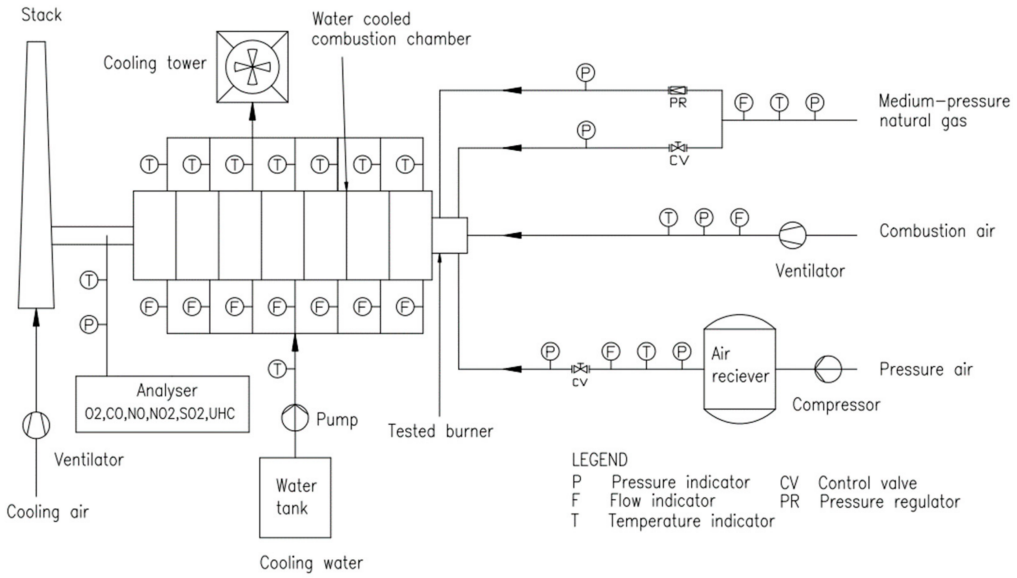

Figure 2. Simplified block diagram of the burner testing facility.

The combustion chamber is equipped with eight inspection windows along the cylindrical part and two inspection windows on the rear side of the chamber opposite the burner, which allows for the observation of the burner flame. The windows along the chamber can also be used to install thermocouples, heat flux probes, etc.

Temperatures inside the combustion chamber can be measured by high-speed water-cooled R-type thermocouples inserted into the inspection holes at each section of the chamber (Figure 3). The data are sent to a Graphtec midi GL220 data logger (Dataq Instruments, Akron, OH, USA).

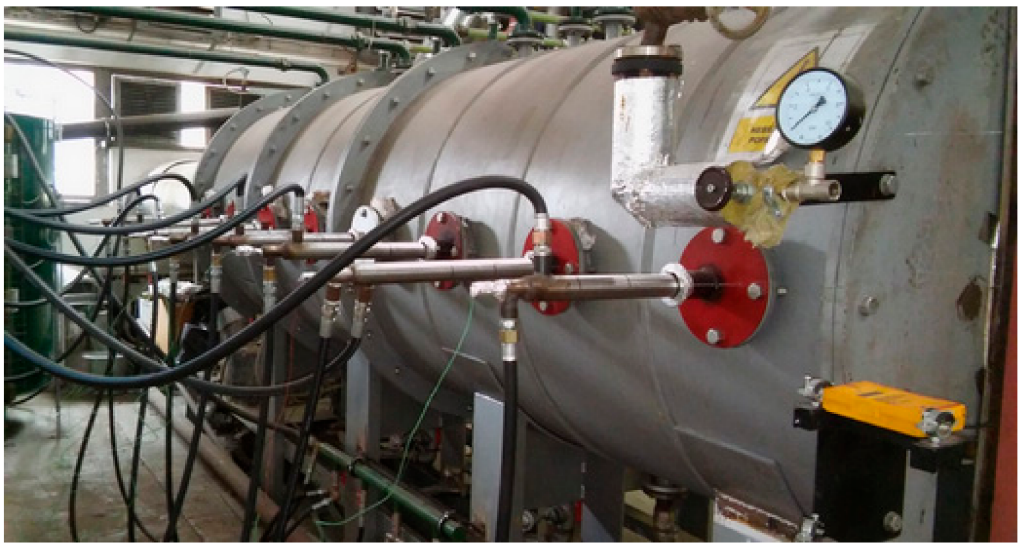

Figure 3. Detail of thermocouples for measuring temperatures in the combustion chamber.

Flue gas is exhausted from the combustion chamber through the flue gas stack, where pressure, flue gas temperature, and flue gas composition are measured. The flue gas analysis and flue gas temperature measurement are provided by the flue gas analyzer TESTO 350-XL (Testo Instruments, Sparta, NJ, USA). The analysis box is equipped with electrochemical sensors for the real-time measurement of O_2, CO, CO_2, NO, and NO_2 concentrations in the dry flue gas. The flue gas temperature is also measured using the thermocouple of type K.

2.2. Burner

The two-staged gas power burner with a maximal thermal input of 1500 kW fired by natural gas (CH_4—98.4 vol%) was used for tests. It is also possible to perform the experiment with different gaseous fuels, with various compositions. We assumed that a major change in the ratio of C_xH_y would not have a big impact on the observed trend in the following sections; although, the presence of H_2 or some other component that intensifies the reaction or presence of fuel bounded nitrogen would result in a change in emissions, namely, NO_x. The three-dimensional model of the used burner can be seen in Figure 4. Burner is equipped with the burner quarl, which has a 300 mm inner diameter, while the outer diameter is 600 mm. The gas inlet is equipped with two circular fields of primary nozzles and a set of secondary nozzles (eight). The nozzles in two circular fields, also called primary, are drilled in the main burner head. In the first field, nozzles with a diameter of 3.0 mm are drilled, the second one consists of eight nozzles each with a diameter of 2.6 mm. The amount of fuel delivered to the primary stage is directly influenced by the exchangeable gas orifice of different diameters. The orifice is located right before the inlet to the main burner head. During the fuel staged combustion regime tests, the primary/total fuel flow ratio was set to 0.28.

The secondary gas distribution is ensured by four nozzles, each with a pitch angle of the head of 30°. At the beveled surface, two nozzles are drilled, each with a diameter of 3.3 mm. The burner is designed to allow for the change in the position of secondary stage nozzles towards the burner tile in both tangential and radial directions. The nozzles are oriented directly towards the burner axis in the reference tangential position. Their orientation can be changed both clockwise in the direction of air swirl motion (corresponding to the positive angle) and counterclockwise (corresponding to the negative angle). In the reference radial distance, the distance of nozzle heads from the burner axis is 180 mm and can be extended by 50 mm. During the tests in the fuel staged combustion regime, the secondary nozzle heads were turned by 20° in the direction of air motion, and their radial distance was set to the maximum, i.e., 230 mm from the burner axis.

The burner was equipped with the flame holder in the form of the swirl generator with eight pitched blades and fixed to the central burner pipe. The swirl generator for our tests had a diameter of 240 mm, and the pitch angle of the swirl generator's blades was 35°. Settings used during the experiment were chosen after prior experiments, chosen parameters were proven best regarding the flame stability and emission. Flame was ignited with the gaseous premixed natural-draught ignition burner with the thermal input of 18 kW. The gas part of the burner is protected by patent No EP 2 853 813 B1.

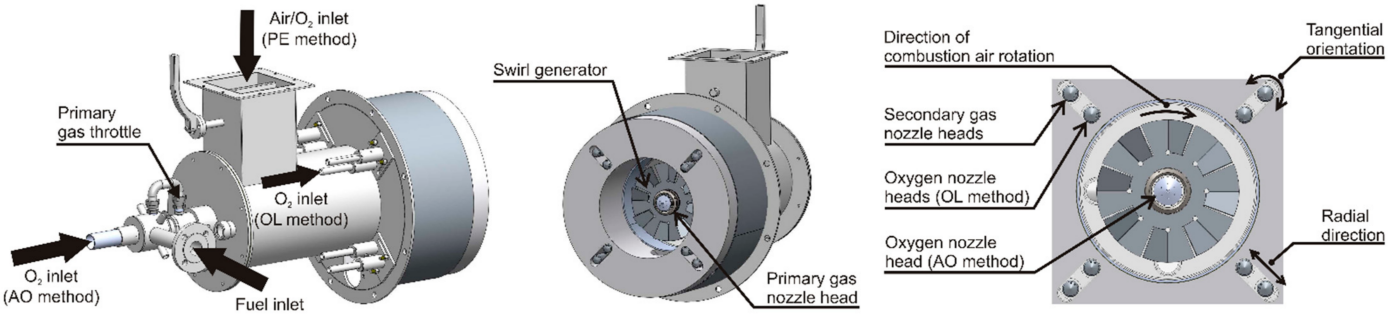

Figure 4. 3D model of the experimental two-staged gas burner.

2.3. Oxygen Supply

The tested OEC methods are illustrated in Figure 4. When using the PE method for the combustion tests, oxygen of high purity was injected into the stream of combustion air. To ensure adequate mixing, oxygen was distributed by the diffuser. The special diffuser, which had several nozzles, was inserted into the stream of the combustion air just before

entering the burner. The maximum oxygen flow rate that the diffuser could handle was 160 Nm^3/h at the overpressure of 6 bar.

For the tests using the AO method, the high-purity oxygen was directed into the flame through the oxygen nozzle head inserted through the center burner pipe. The oxygen balance necessary for complete combustion was supplied to the burner via the atmospheric air. The oxygen nozzle head was designed for the maximum oxygen flow rate of 120 Nm^3/h at the overpressure of 6 bar.

For the tests using the OL method, the high-purity oxygen was injected in the secondary stage of combustion through four oxygen nozzle heads located near the secondary gas nozzle heads. The radial distance of oxygen nozzle heads from the burner axis was set to the minimum of 180 mm, and the heads were turned by 30° clockwise. The pitch angle of each head was 20°. The maximum oxygen flow rate through all heads was set to 150 Nm^3/h at the overpressure of 6 bar.

2.4. Planning of Combustion Tests

The experimental matrix is presented in Table 1. The symbol • indicates that the test was carried out for the set overall oxygen concentration in the oxidant and combustion regime. For instance, "PE one-staged" stands for the combination of premix enrichment OEC method and one-staged fuel combustion (fuel is distributed only through primary nozzles), the whole "PE two-staged" stands for the combination of premix enrichment OEC method and two-staged fuel combustion (fuel is distributed through both primary and secondary nozzles). All tests were performed at the burner thermal input of 750 kW. The target oxygen concentration in the dry flue gas was kept at 3% by volume for all tests. The pressure in the combustion chamber was kept around -100 Pa.

Table 1. Plan of combustion tests.

Tested—Combustion Regime	Flow Rate of O_2 (Nm^3/h)/Overall O_2 Concentration in the Oxidant (%)								
	0/21	**5/21.5**	**10/22**	**20/23.1**	**30/24.3**	**40/25.6**	**60/29**	**80/33**	**100/38**
TEST A									
Premix enrichment									
PE one-staged	•	•	•	•	•	•	•	•	-
PE two-staged	•	•	•	•	•	•	•	•	•
Air-oxy/fuel									
AO one-staged	•	•	•	•	•	•	•	•	•
AO two-staged	•	•	•	•	•	•	•	•	•
O_2 ***lancing***									
OL one-staged	•	•	•	•	•	•	•	-	-
OL two-staged	•	•	•	•	•	•	•	•	-
TEST B									
Premix enrichment									
PE one-staged	•	-	-	•	-	•	-	•	-
PE two-staged	•	-	-	•	-	•	-	•	-
Air-oxy/fuel									
AO one-staged	•	-	-	•	-	•	-	•	-
AO two-staged	•	-	-	•	-	•	-	•	-
O_2 ***lancing***									
OL one-staged	•	-	-	•	-	•	-	-	-
OL two-staged	•	-	-	•	-	•	-	•	-
TEST C									
Premix enrichment									
PE one-staged	•	-	-	•	-	•	•	•	-
PE two-staged	•	-	-	•	-	•	•	•	-
Air-oxy/fuel									
AO one-staged	•	-	-	•	-	•	•	•	-
AO two-staged	•	-	-	•	-	•	•	•	-
O_2 ***lancing***									
OL one-staged	•	-	-	•	-	•	•	-	-
OL two-staged	•	-	-	•	-	•	•	•	-

The experimental investigation was aimed to assess the influence of OEC methods, varying oxygen concentration from 21% to 38% and fuel staging on the NO_x and CO emissions, flue gas temperature, heat flux distribution to the combustion chamber wall lengthwise the flame, in-flame temperatures distribution in the horizontal symmetry plane of the combustion chamber, and the stability of flame. As for the PE tests, the oxygen concentration between 21% and 38% matches directly the oxygen concentration in the incoming combustion air. On the other hand, in the tests using the AO and OL methods, the oxygen was not mixed with the combustion air in the air supply pipe, and hence the oxygen concentration in the incoming air was always 21%. Thus, the 21–38% oxygen concentration expresses the overall oxygen concentration as if both air and oxygen streams (injected directly into the combustion chamber) are mixed.

Three types of tests were the subject of our study. In the first test, denoted as TEST A, the quality of combustion and flame characteristics were investigated. We measured the concentrations of NO_x and CO emissions in flue gas, flue gas temperature at the outlet of the combustion chamber, and observed the burning stability of oxygen-enhanced flames. Before the experiments, the combustion chamber was set into a steady thermodynamic state. The condition necessary for the beginning of data collection was in accordance with the burner testing standards, i.e., the flue gas temperature must not exceed the interval of 10 °C within 30 min.

The second test, denoted as TEST B, focused on evaluating and comparing local wall heat fluxes into the walls of the chamber's sections. The data collection started after the combustion chamber was set into the steady thermodynamic state defined as if both the flue gas temperature (maximum allowed change within 30 min is 10 °C) and the values of local wall heat fluxes (continuously evaluated by the control system of the testing facility) are steady.

In the third test, denoted as TEST C, the in-flame temperatures in the horizontal symmetry plane of the combustion chamber were measured using seven water-cooled platinum/platinum-rhodium (containing 13% of rhodium) thermocouples of type R installed through the inspection windows. The in-flame temperatures were measured at distances of 0, 10, 20, 30, 40, and 45 cm from the axis of the combustion chamber. The data collection started when the same steady conditions as for TEST A were reached. However, unlike TEST A, TEST B, and TEST C were carried out only for selected overall oxygen concentrations (see Table 1). Concentrations were chosen according to the results given by Design of Experiment (DOE), which was used to eliminate redundant measurements to optimize the time and consumption of the fuel and oxidizer.

3. Results and Discussion

Results gained during the TEST A are described in Sections 3.1–3.7, results obtained during TEST B are described in Section 3.8, and, finally, results obtained during the TEST C are discussed in Section 3.9.

3.1. NO_x Emissions

Figure 5 compares the trends of NO_x concentrations (mg/Nm^3) as a function of overall oxygen concentration. The concentrations of NO_x were calculated from the measured concentrations of NO (measured in units (ppm)) and NO_2 (measured in units (ppm)), and the values were corrected to 3% O_2 level in the dry flue gas. The ratio between the two nitrogen oxide components was NO 95% and NO_2 5%. Generally, the significant proportion of NO_x produced during combustion was thermal NO_x, which was directly associated with higher flame temperature peaks due to higher O_2 concentrations in the oxidizer [2,17].

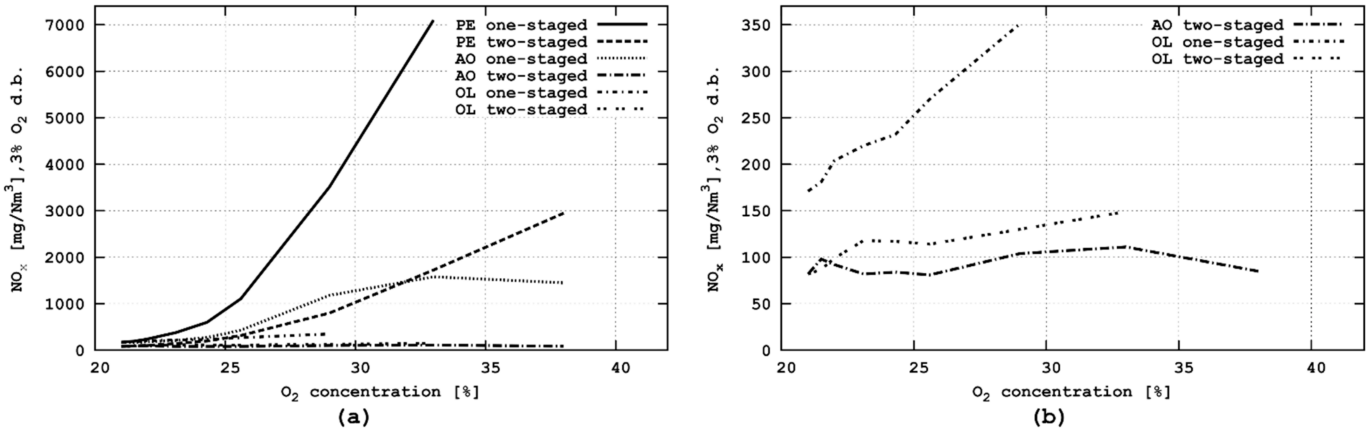

Figure 5. (**a**) Effect of oxygen concentration, OEC method, and combustion regime on the NO_x emissions. (**b**) The detail for the AO two-staged, OL one-staged, and OL two-staged regime.

3.2. Premix Enrichment

A significant increase in NO_x emissions was observed when the oxygen enrichment increased for both one-staged and two-staged fuel combustion regimes. This increase appears to be approximately exponential and is substantially affected by the in-flame temperature peaks. Due to this, even a minor variation in the flame temperature accelerated the NO_x formation. In the one-staged regime, the NO_x emissions increased sharply from 170 to 7100 mg/Nm^3 as the O_2 concentration in the combustion air increased from 21% to 33%. Further air enrichment was unacceptable for the following two reasons. Firstly, the measured NO values were beyond the measuring range of the NO sensor. Secondly, the swirl generator blades and the burner quarl became red-hot due to very high temperatures at the burner tile and a decrease in the flow rate of combustion air working as a cooler of the burner quarl.

On the other hand, when the two-staged fuel combustion regime was used as the NO_x reducing technique, the increase in NO_x emissions was not as steep as their increase in the one-staged fuel combustion regime because the reaction of fuel with oxygen was staged. Furthermore, the flame temperature peaks near the burner exit were reduced compared to the one-staged fuel combustion regime (see temperature distributions in Section 3.9). Therefore, the NO_x emissions rose gradually from 80 to 3000 mg/Nm^3 as the oxygen concentration increased from 21% to 38%. It should be also noticed that the NO_x emissions reached only 1700 mg/Nm^3 at 33% O_2, i.e., by ca. four times less than the emissions in the PE one-staged regime with the same oxygen concentration. For this regime, further air enrichment would be possible with respect to the construction of the swirl generator and the burner quarl because no overheating was observed. Additionally, the NO concentration was still within the measuring range of the NO sensor. However, the NO_x concentrations were too high above the specific emission limit valid for stationary sources with the thermal input in the range between 0.3 and 50 MW (for the Czech Republic, the current limit is 200 mg/Nm^3); thus, there does not seem to be a potential for industrial applications.

3.3. Air-Oxy/Fuel Combustion

The tests using the AO method did not show any dramatic increase in NO_x emissions compared to the PE method. The maximum reachable operating flow rate of oxygen in AO tests was 100 Nm^3/h, corresponding to the overall oxygen concentration of 38%. However, the influence of a higher oxygen flow rate could not be investigated because the flame became unstable, and the flashback inside the burner was observed.

When the AO method was combined with the one-staged fuel combustion regime, the NO_x emissions increased gradually to 1500 mg/Nm^3 as the overall oxygen concentration increased to 33%, as shown in Figure 5a. However, it was observed that further increase in O_2 flow rate slightly reduces NO_x. The reason is that a significant portion of the fuel is combusted in the flame core, whereto the high-purity oxygen is injected. Hence, the flame core is very rich in oxygen and poor in nitrogen. This, in turn, results in low NO_x, although the flame temperature peaks are very high. This observation was observed also in results obtained by CFD analysis by Prieler et.al. [18]. CFD analysis used data gathered during the first series of experiments as described in precedent article [15]. The balance of fuel is then combusted downstream of this dominant combustion zone at lower temperatures that are not favorable for the thermal NO formation. Therefore, it can be assumed that further increase in O_2 concentration can lower NO_x because less N_2 is available to form NO_x. However, retrofitting of the current burner geometry would be necessary to stabilize the flame.

Auspicious results were obtained using the AO method in combination with fuel staging. The effect of oxygen concentration on NO_x emissions can be seen in Figure 5b. The NO_x concentration fluctuated mostly around 100 mg/Nm^3 and reached a maximum of 110 mg/Nm^3 at 33% O_2. The reason was that a part of the fuel was directed into the primary combustion zone while the balance of the fuel was directed into the secondary combustion zone. This made the primary zone fuel-lean, i.e., less conducive to NO_x formation compared to the one-staged fuel combustion regime [6]. The excessive O_2 from the primary zone was used to complete the combustion of the secondary fuel. The peak flame temperature was much lower in the fuel staged case because the combustion is staged over a particular distance (see temperature distributions in Section 3.9). Consequently, lower temperatures contributed to the reduction in NO_x emissions. Further increase in O_2 concentration seems to have the same effect as observed in the AO one-staged tests, i.e., the NO_x reduction.

3.4. Oxygen Lancing

Based on our research measurements, the method of oxygen lancing was distinguished from previous OEC methods by lower NO_x formation both for the one-staged and two-staged fuel combustion regime. The effect of oxygen concentration on NO_x emissions is shown in detail in Figure 5b. When the OL method was used in combination with the one-staged and two-staged fuel combustion regime, the oxygen concentration reached 29% and 33% at the maximum, respectively. However, once this oxygen level was exceeded, the flame became very unstable and pulsated due to the lack of oxygen in the flame core.

In the one-staged fuel combustion regime, the NO_x rose linearly and reached the maximum of 350 mg/Nm^3 at 29% O_2, which is significantly lower in comparison with the PE method (3500 mg/Nm^3 at 29% O_2) and AO method (1180 mg/Nm^3 at 29% O_2). This can be explained by the high-purity oxygen being fed not to the primary combustion zone but downstream the flame through the OL oxygen nozzle heads (Figure 4). Due to this, the temperature peaks in the flame core were lower than with PE and AO methods (see also Section 3.9), which suppressed the NO_x formation.

When the fuel supply was staged (OL two-staged regime), lower temperature peaks in the flame core were observed, too. Moreover, the temperature distributions were relatively uniform in the flame region, and the flue gas temperature decreased drastically (Figure 6) with a parallel increase in the heat transfer rate. Therefore, the NO_x emissions rose gradually from 80 to 150 mg/Nm^3 as oxygen concentration increased from 21% to 33%.

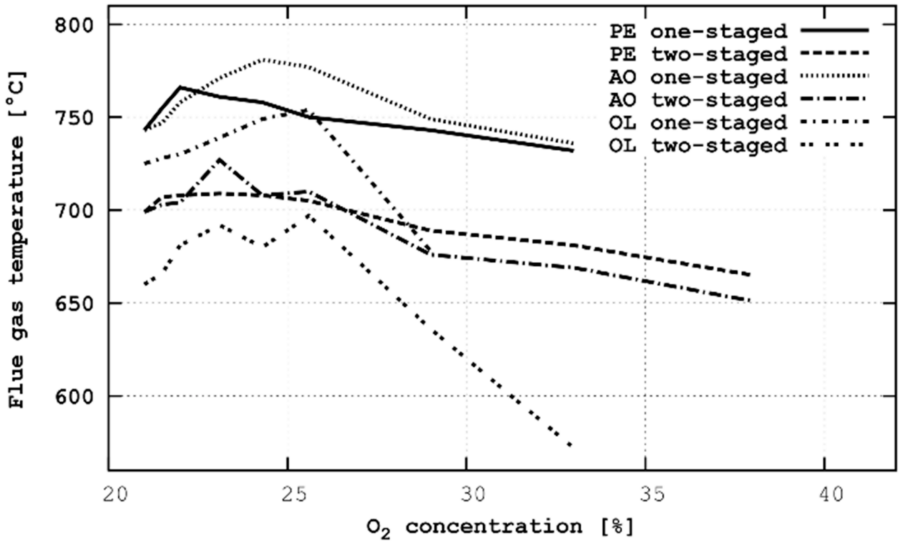

Figure 6. Effect of oxygen concentration, OEC method, and combustion regime on the flue gas temperature.

Summing up, when the PE and AO methods were combined with the one-staged fuel combustion regime and the PE method in combination with fuel staging, the NO_x emissions increased significantly with increasing overall oxygen concentration. Therefore, their utilization for industrial applications can be considered only for minor oxygen enrichment rates up to 2%. A slightly higher increase in NO_x was observed in the case of the OL one-staged method; however, NO_x was still above the specific emission limit valid for stationary sources with the thermal input ranging from 0.3 to 50 MW. In terms of NO_x emissions, AO and OL methods combined with the two-staged fuel combustion regime seem to be appropriate options; the concentration of NO_x was deeply below the specific emission limit for all investigated oxygen concentrations. The obtained results comply with the results reported by Wu et al. [7], Persis et al. [19], and Abdelaal et al. [20]. On the other hand, Merlo et al. [8] did not observe such a steep increase in NO_x.

3.5. CO Emissions

During the measurements, the measured concentrations of CO were lower than 5 mg/Nm^3 for all performed tests indicating the complete combustion. This is again in good agreement with the results of Wu et al. [7]. On the other hand, Merlo et al. [8] observed very high CO emissions (more than 2000 ppm) at low oxygen enrichment rates, which could be caused by insufficient mixing of fuel with oxidant.

3.6. Flue Gas Temperature

Figure 6 shows the variation in the flue gas temperature as a function of overall oxygen concentrations and OEC methods. The flue gas temperature slightly increased as O_2 concentration increased to 23–25%. However, further increase in the O_2 concentration caused a decrease in the flue gas temperature. For example, with the increase in the oxygen enrichment rate, the flue gas temperature dropped from 730 to 650 °C in the AO two-staged regime and from 700 to 570 °C in the OL two-staged regime.

A decreasing trend of flue gas temperature was affected by a decreasing concentration of nitrogen, which only absorbs heat and carries energy away with flue gases. Consequently, this effect is associated with the increasing radiant heat flux from the hot flue gas to the combustion chamber's wall (Figure 7) and increasing heat transfer efficiency (Figure 8).

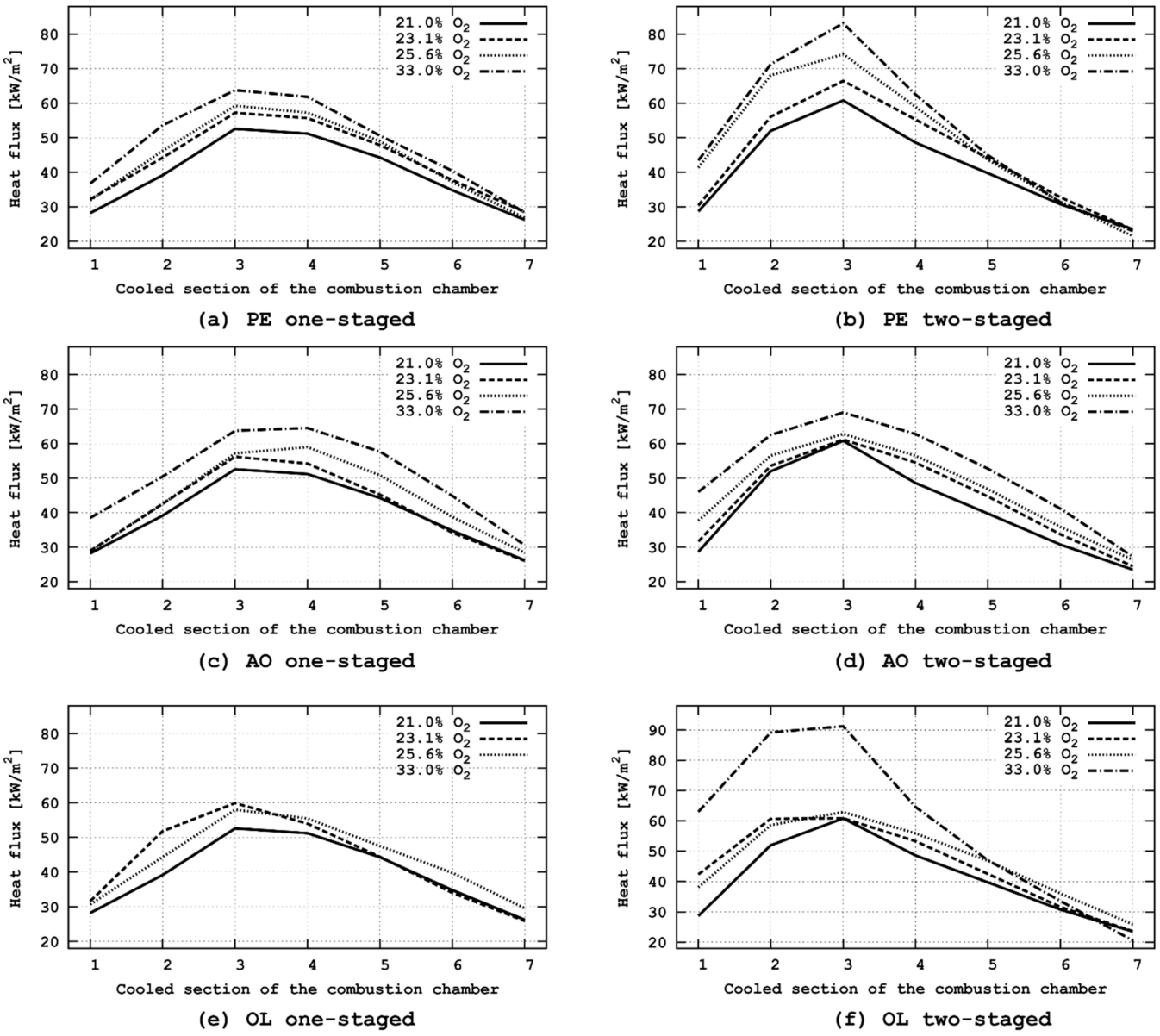

Figure 7. Heat flux distributions lengthwise the combustion chamber for various combustion regimes.

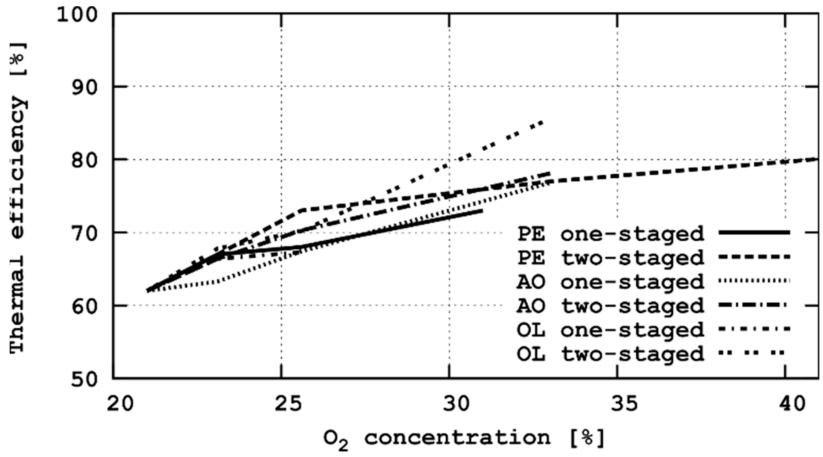

Figure 8. Effect of overall oxygen concentration on the heat transfer efficiency.

3.7. Flame Stability

The air/fuel flames were characterized by the blue flame core and the yellow-red flame tips. Furthermore, the core of oxygen-enhanced flames turned yellower as the O_2 concentration increased. In general, observed OEC flames were more luminous/radiant than the air/fuel flame. Moreover, the OEC flame's emissivity is higher because of the higher concentrations of carbon dioxide and water vapor, the gases that radiate in the flame (nitrogen has no such effect in the flame, and thus it acts as a ballast).

The flame stability of OEC flames depended on: (1) the OEC method, i.e., the location of high-purity oxygen injection; (2) fuel combustion regime, i.e., the one-staged or two-staged fuel supply; and (3) overall oxygen concentration in the oxidant, i.e., the volume flow rate of combustion air and high-purity oxygen. These three aspects influence the flame stability parameters, such as the mixing intensity of fuel with combustion air and high-purity oxygen, creating the reaction zones, and the flame speed. The flames produced using the PE method were stable and sharp for all investigated oxygen concentrations. Further oxygen enrichment seemed to be desirable in terms of flame stability, but it was undesirable in terms of NO_x and the burner construction.

On the other hand, the flame instabilities were observed with flames produced using AO and OL methods. In both methods, the oxygen is injected directly into the combustion chamber, while the balance of oxygen is ensured by the combustion air (21% O_2) supplied through the burner body. Hence, the flow rate of combustion air was reduced with the increasing overall oxygen concentration, which subsequently caused the reduction in the mixing intensity, and the burner velocity became more remarkable than the outlet velocity of air. Moreover, in OL tests, the instability was also caused by the substantial shortage of oxygen in the primary combustion zone (i.e., the zone was rich in fuel) serving as a stabilizer for the secondary combustion zone, as the flow rate of injected high-purity oxygen was rising.

3.8. Heat Flux Distribution

The burner testing facility measures the heat flux based on the heat absorbed by the cooling water in each chamber's section. The flame-facing area of the first and seventh chamber's sections is reduced due to the insulation of the front and rear sides of the chamber. Thus, the first section is 0.4 m (not 0.5 m) long, the flame-facing area is 1.26 m^2, the length of the seventh section is shortened to 0.9 m, and the flame-facing area is 2.83 m_2. The sections 2–6 are 0.5 m long, and the flame-facing area is 1.57 m^2. Since the sections of the combustion chamber represent the calorimetric cells [21], the heat flux to the i-th chamber's section wall can be determined based on the measured volumetric flow rate of cooling water, inlet water temperature inside the section, outlet water temperature outside the section, and the flame-facing area using the Equation (1) [22]:

$$\dot{q}_i = \frac{\dot{V}_i \cdot \rho_i \cdot c_{p,i} \cdot \Delta t_i}{1000 \cdot 3600 \cdot A_i} = \frac{\dot{V}_i \cdot \rho_i \cdot c_{p,i} \cdot (t_{OUT,i} - t_{IN,i})}{1000 \cdot 3600 \cdot A_i} \quad \text{for } i = 1, 2, \ldots, 7 \tag{1}$$

In Equation (1), the heat flux is (kW/m^2), the volumetric flow rate of cooling water is (m^3/h), the water density is (kg/m^3), the specific heat capacity is (J/(kg·K)), the temperature difference is (°C) between the outlet and inlet temperature of cooling water, and the flame-facing area of the *i*-th section is (m^2). The water density and specific heat capacity were assumed to be constant in the whole volume of each chamber's section and were calculated using the approximation formulas Equation (2) [22] and Equation (3) [22], where

$$\rho_i = 1006 - 0.26 \cdot \frac{\hat{t}_i}{2} - 0.0022 \cdot \left(\frac{\hat{t}_i}{2}\right)^2 \quad \text{for } i = 1, 2, \ldots, 7 \tag{2}$$

$$c_{p,i} = 4210 - 1.363 \cdot \frac{\hat{t}_i}{2} + 0.014 \cdot \left(\frac{\hat{t}_i}{2}\right)^2 \quad \text{for } i = 1, 2, \ldots, 7 \tag{3}$$

In Equations (2) and (3), $\hat{t}$ is inlet temperature (°C). The heat flux profiles are shown and compared in Figure 7. The trend curves of the heat flux are characterized by a very similar shape for all investigated O_2 concentrations and all combustion regimes. The individual curves are shifted upwards as the oxygen concentration increases, which is in agreement with the results of Horbaniuc et al. [10]. The maximum heat flux was reached in the third section of the combustion chamber for all tests. It can be seen that with increasing O_2 concentration, more heat is released from the hot flue gas to the walls of the chamber's sections because less energy is wasted for N_2 heating, and the radiative heat transfer rate is enhanced with the higher concentrations of CO_2 and H_2O and with the increased residence time of the hot flue gas in the chamber.

The heat transfer efficiency, defined as the ratio of the furnace heat flux (heat flux to the furnace wall or heated load) to the heat delivered with fuel, is shown in Figure 8. The heat supplied with the combustion air and high-purity oxygen was not considered here. The figure shows that even minor oxygen enrichment rapidly increases the heat transfer efficiency. Therefore, low-level oxygen enrichment is commonly used in retrofit applications because an incremental increase in efficiency is crucial.

The heat transfer efficiency of the combustion process was increased from 60% at 21% O_2 to 78% at 33% O_2 (or even to 85% at 33% O_2 for OL two-staged regime), i.e., more heat is available for the overall process, which brings about two positive results. Firstly, increasing the oxygen concentration can save energy, i.e., it can reduce fuel consumption when less fuel is required for a particular unit of production because of the improvement in available heat. Secondly, the heat transfer surfaces (e.g., process tubes in boilers) can be diminished if the boiler's heat output is required to be kept at the same level. Therefore, the cost of process tubes can also be significantly cut down.

3.9. In-Flame Temperatures

Another aim of the experimental part of this paper was to investigate the temperature distribution in the chamber for all three setups. The temperatures were measured in the flame by R-type thermocouples described in Section 2.1. The burner geometry was taken into account and it was presumed that the temperature distribution is symmetric concerning a vertical plane passing through the axis of the cylindrical chamber. Mainly for this reason, measurement of the temperatures took part only in one half of the chamber. As introduced in Section 2.1, there are eight observation windows on one side of the chamber. The distance between these holes is 0.5 m. In each of these holes, a thermocouple was placed and moved in the radial direction. The temperatures were measured in distances of 5, 10, 20, 30, 40, and 50 cm from the inner shell. The chamber was designed as circular with an inner diameter of 1 m. The last position (50 cm) was situated directly on the axis of the experimental chamber. The data for 60 s in each position at a sampling frequency of 1 s were collected. Afterward, the arithmetic mean was calculated from this data set. For every single setup, 48 values were obtained (eight R-type thermocouples, six positions). For the visualization simple script was written in Python programming language was used.

Figures 9–11 represent the in-flame temperature distributions measured in the horizontal symmetry plane of the combustion chamber. As expected, high-temperature zones are located near the burner region. The temperature near the burner exit rose most significantly for the PE one-staged regime (Figure 9) due to less nitrogen acting as a diluent, which resulted in the highest NO_x. The temperature was 1100–1300 °C at 21% O_2, compared with 1300–1500 °C at 33% O_2. On the other hand, the temperature field in the lower part of the combustion chamber was highly uniform for the AO two-staged regime (Figure 10) and the OL two-staged regime (Figure 11). For these combustion regimes, the temperature ranged between 1100 and 1200 °C at all investigated oxygen concentrations (21–38% O_2). Due to lower temperatures and fuel staging, the NO_x formation is suppressed for these combustion regimes, and simultaneously the heat transfer efficiency is increased by ca. 20%.

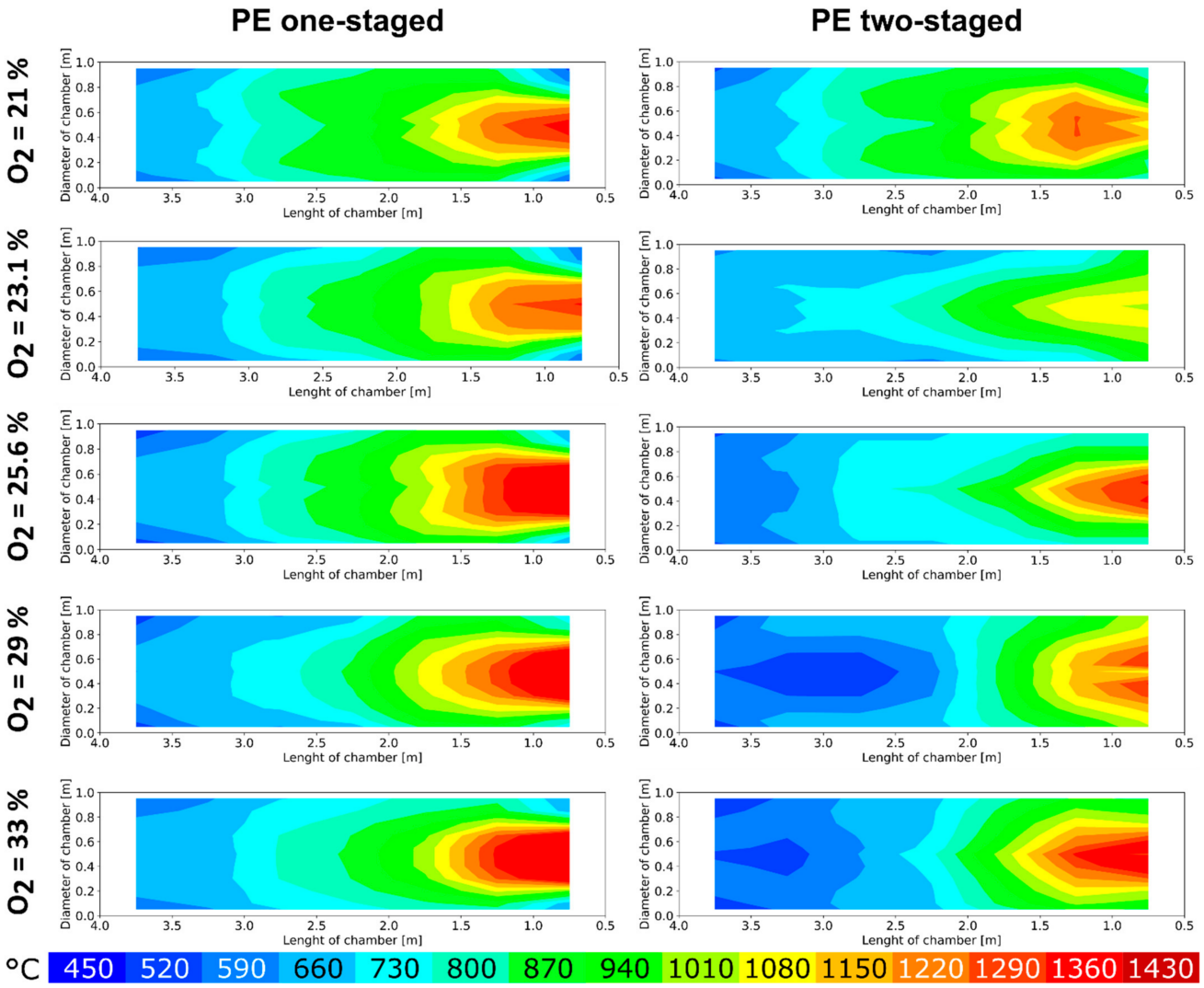

Figure 9. In-flame temperature distributions for the PE method.

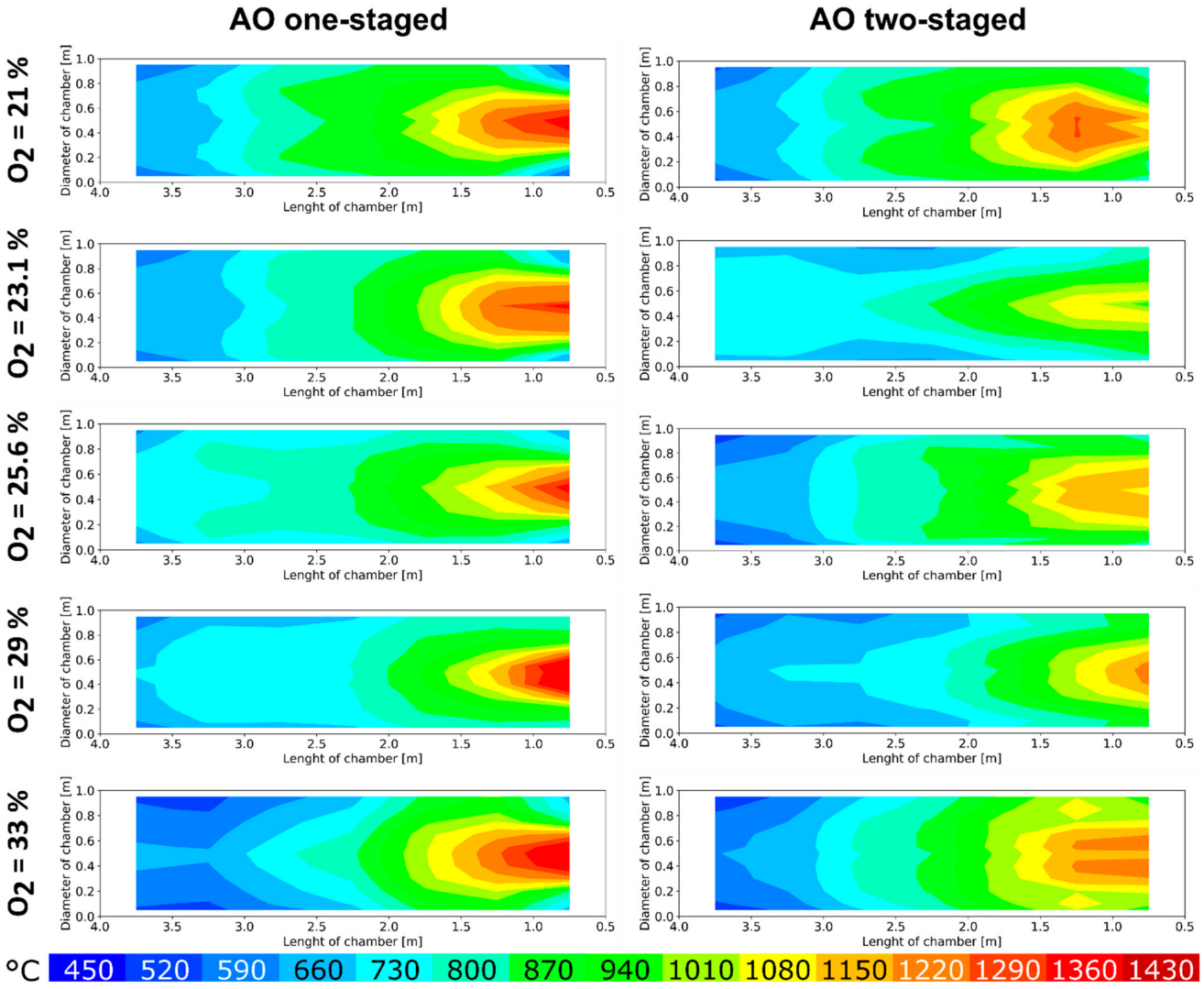

Figure 10. In-flame temperature distributions for the AO method.

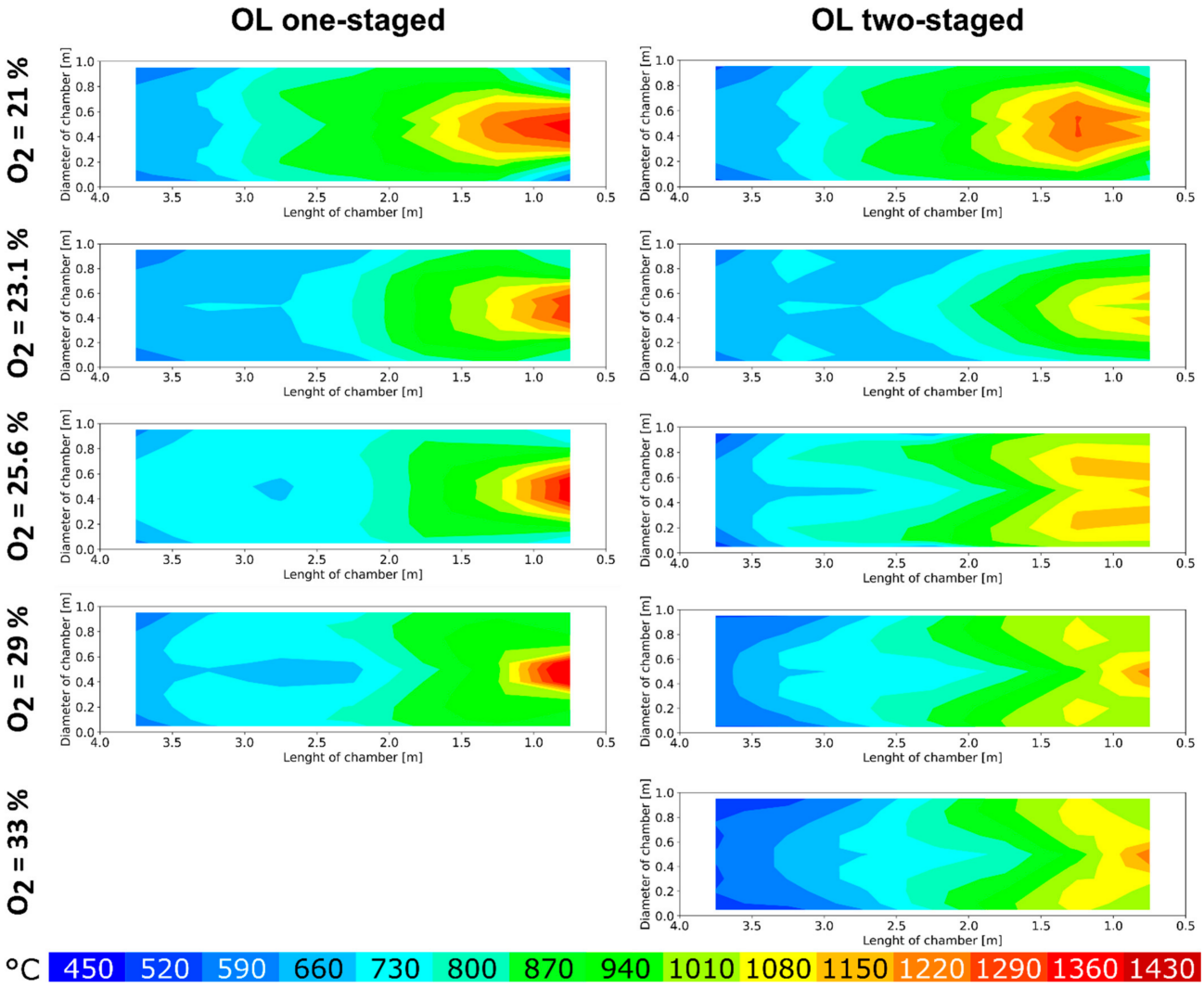

Figure 11. In-flame temperature distributions for the OL method.

4. Error Analysis

Experimental measurements are affected by the uncertainties that arise from the inaccuracies of used instrumentation. Measurements of NO and NO_2 concentrations, the measuring ranges, accuracies, and resolutions of the sensors are given in Table 2. The technical parameters of the sensors of the water-cooling system, including the turbine flow meter and resistance thermometers, are summarized in Table 3. The relative errors for NO_x emissions and heat fluxes were calculated using the uncertainty propagation method [23,24].

Table 2. Technical parameters of the NO and NO_2 sensors of the flue gas analyzer.

Probe Type	Range	Accuracy ±1 Digit	Resolution
NO	(0–3000) ppm	• ±5 ppm in the range (0–99) ppm • ±5% of the measured value in the range (100–2000) ppm	1 ppm
NO_2	(0–500) ppm	• ±5 ppm in the range (0–99) ppm • ±5% of the measured value in the range (100–500) ppm	0.1 ppm

Table 3. Technical parameters of the sensors of the water-cooling system.

Probe Type	Sensor	Range	Accuracy ±1 Digit
Temperature	Rawet PTP50J Pt100/B (Rawet, Blansko, Czech Republic)	(0–100) °C	±0.3% of measuring range
Flow rate	Sensus Type 420 S Qn 10 (Sensus, Morrisville, NC, USA)	(0.15–40) m^3/h	±0.5% of measured value

4.1. NO_x Emissions

The concentrations of NO_x emissions (mg/Nm^3) were calculated based on the measured concentrations of NO (ppm) and NO_2 (ppm). The standard deviation of NO_x is calculated according to the following Equation (4):

$$\sigma_{NO_x} = \sqrt{\sigma_{NO}^2 + \sigma_{NO_2}^2} \quad (4)$$

where σ_{NO} and σ_{NO2} are the standard deviations of measured NO converted to NO_2 equivalent, and measured NO_2, respectively. The relative errors are summarized in Table A1 in Appendix A. The highest relative errors from 10% to 18% were obtained at the configurations where the NO_x concentrations were below 150 mg/Nm^3. These configurations include the PE, AO, and OL methods combined with fuel-staged combustion. The relative errors for other configurations ranged from 5% to 10%.

4.2. Heat Fluxes

When TEST B was performed, the flow rate of cooling water through each section was decreased to its minimum, consequently reducing the uncertainty of the heat flux measurement. Due to a lower flow rate of cooling water, the outlet temperature increases, and hence the difference between the outlet and inlet temperature also increases. Based on the calculation of uncertainty propagation, the heat flux measurement uncertainty is inversely proportional to the temperature difference. Therefore, the standard deviation of calculated heat fluxes holds the Equation (5) [22]:

$$\sigma_{\dot{q}_i} = \dot{q}_i \cdot \sqrt{\left[\left(\frac{\sigma_{V_i}}{V_i}\right)^2 + \frac{\sigma_{t_{OUT,i}}^2 + \sigma_{t_{IN}}^2}{\Delta t_i^2}\right]} \text{ for } i = 1, 2, \ldots, 7 \quad (5)$$

where $\sigma_{\dot{V}_i}$ is the standard deviation of the flow meter, $\sigma_{t_{OUT,i}}$ and $\sigma_{t_{IN}}$ are the standard deviations of thermocouples at the section outlet and inlet, respectively. The calculated relative errors are summarized in Table A2 in Appendix A. The maximum relative error was within ±5% for the first section and within ±3% for other sections. The higher relative error in the first section arises because the heat transfer rate to the wall of the first section is lower than to the other sections, and hence the temperature difference between the outlet and inlet temperature of cooling water is also lower than for other sections. As explained above, this increases the relative error of the heat flux.

5. Conclusions

The present study describes three types of combustion tests carried out to investigate the effects of three OEC methods, the overall oxygen concentration in the range of 21–38% and combustion regime on combustion parameters such as NO_x and CO emissions, flue gas temperature, in-flame temperatures distribution in the horizontal symmetry plane of the combustion chamber, heat flux to the combustion chamber wall, and the stability of flame. The general conclusions drawn from the results of this research can be summarized as follows:

1. The NO_x emissions increased distinctly owing to a higher furnace temperature as the oxygen concentration increased during the tests of the PE method. For example, when the oxygen concentration increased from 21% to 33%, the NO_x concentration increased by more than 40 times, and by 20 times when the one-staged and two-staged combustion regimes were used, respectively. However, much better results were achieved during the tests using the AO and OL methods in combination with fuel staging, when NO_x was below 110 mg/Nm^3 and 150 mg/Nm^3 for all investigated oxygen enrichment rates, respectively.
2. The flue gas temperature decreased with the increasing overall oxygen concentration. A decrease in flue gas temperature was due to a decreasing nitrogen concentration in the oxidizer and increasing radiant heat flux.
3. The radiative heat transfer rate was enhanced as the overall oxygen concentration increased. The recoverable heat at 33% O_2 was approximately 20% higher than at 21% O_2.
4. Generally, the oxygen-enhanced flames were more luminous than the air/fuel flames. The flames produced using the PE method were stable at all investigated oxygen concentrations. However, the flame instabilities and flashback were observed when the AO and OL methods were tested.
5. For the PE method, increasing oxygen concentration led to a higher temperature gradient of non-uniform temperature distribution in the horizontal plane of symmetry of the combustion chamber. On the other hand, AO and OL methods combined with fuel-staging seem to be beneficial due to a highly uniform temperature field.

Author Contributions: Conceptualization, P.S. and I.H.; methodology, I.H.; software, J.B.; validation, Z.J. and J.B.; formal analysis, I.H.; investigation, P.S.; resources, J.B.; data curation, Z.J.; writing—original draft preparation, P.S.; writing—review and editing, I.H.; visualization, J.B.; supervision, L.K. and Z.J.; project administration, Z.J. and P.S.; funding acquisition, P.S. All authors have read and agreed to the published version of the manuscript.

Funding: This research was funded by the Czech Ministry of Education, Youth, and Sports/EU Operational Programme Research, Development and Education, grant no. CZ.02.1.01/0.0/0.0/16_026/0008413 "Strategic partnership for environmental technologies and energy production". Furthermore, the authors gratefully acknowledge the financial support provided by the Technology Agency of the Czech Republic (TACR) within the research project National centers of competence, specifically through the project National Centre for Energy (TN1000007).

Data Availability Statement: Please contact the authors.

Conflicts of Interest: The authors declare no conflict of interest.

Abbreviations

Symbols

$\dot{q}_i$	Heat flux to the wall of the i-th chamber's section	(kW/m^2)
$\dot{V}_i$	Volumetric flow rate of cooling water through the i-th chamber's section	(m^3/h)
ρ_i	Density of cooling water in the i-th chamber's section	(kg/m^3)
$c_{p,i}$	Specific heat capacity of cooling water in the i-th chamber's section	(J/(kg·K))
Δt_i	Temperature difference between outlet and inlet temperature of cooling water	(°C)
$t_{OUT,i}$	Outlet temperature of cooling water out of the i-th chamber's section	(°C)

$t_{IN,i}$	Inlet temperature of cooling water in the *i*-th chamber's section	(°C)
A_i	Flame-facing area of the *i*-th chamber's section	(m^2)
σ_{NO_x}	Standard deviation of calculated NOx	(mg/Nm^3)
σ_{NO}	Standard deviation of measured NO converted to NO_2 equivalent	(mg/Nm^3)
σ_{NO_2}	Standard deviation of measured NO_2	(mg/Nm^3)
$\sigma_{\dot{q}_i}$	Standard deviation of calculated heat flux to the wall of the *i*-th chamber's section	(kW/m^2)
$\sigma_{\dot{V}_i}$	Standard deviation of water flow rate through the *i*-th chamber's section	(m^3/h)
$\sigma_{t_{OUT,i}}$	Standard deviation of outlet temperature of cooling water out of the *i*-th chamber's section	(°C)
$\sigma_{t_{IN,i}}$	Standard deviation of inlet temperature of cooling water in the *i*-th chamber's section	(°C)

Acronyms

OEC	Oxygen-enhanced combustion
PE	Premix enrichment
AO	Air-oxy/fuel combustion
OL	Oxygen lancing

Appendix A

Table A1. Error analysis for the NO_x emissions.

Trial—Combustion Regime	The Flow Rate of O_2 [Nm^3/h]	Overall O_2 Conc. [%]	NO_x [mg/Nm^3]	Relative Error [%]
PE one-staged	0	21.0	171	8.5
PE one-staged	5	21.5	195	7.5
PE one-staged	10	22.0	242	6.4
PE one-staged	20	23.1	381	5.5
PE one-staged	30	24.3	600	5.1
PE one-staged	40	25.6	1107	5.0
PE one-staged	60	29.0	3511	4.9
PE one-staged	80	33.0	7099	4.9
PE two-staged	0	21.0	82	17.7
PE two-staged	5	21.5	92	15.7
PE two-staged	10	22.0	105	13.8
PE two-staged	20	23.1	145	10.0
PE two-staged	30	24.3	199	7.3
PE two-staged	40	25.6	316	5.7
PE two-staged	60	29.0	800	5.1
PE two-staged	80	33.0	1724	4.9
PE two-staged	100	38.0	2949	4.9
AO one-staged	0	21.0	171	8.5
AO one-staged	5	21.5	168	8.6
AO one-staged	10	22.0	181	8.0
AO one-staged	20	23.1	212	6.9
AO one-staged	30	24.3	275	6.1
AO one-staged	40	25.6	434	5.4

Table A1. *Cont.*

Trial—Combustion Regime	The Flow Rate of O_2 [Nm^3/h]	Overall O_2 Conc. [%]	NO_x [mg/Nm^3]	Relative Error [%]
AO one-staged	60	29.0	1181	5.0
AO one-staged	80	33.0	1579	4.9
AO one-staged	100	38.0	1450	5.0
AO two-staged	5	21.5	98	14.8
AO two-staged	10	22.0	92	15.8
AO two-staged	20	23.1	82	17.7
AO two-staged	30	24.3	84	17.2
AO two-staged	40	25.6	81	18.0
AO two-staged	60	29.0	104	13.9
AO two-staged	80	33.0	111	13.1
AO two-staged	100	38.0	85	17.1
OL one-staged	0	21.0	171	8.5
OL one-staged	5	21.5	181	8.0
OL one-staged	10	22.0	204	7.1
OL one-staged	20	23.1	220	6.8
OL one-staged	30	24.3	232	6.6
OL one-staged	40	25.6	270	6.3
OL one-staged	60	29.0	351	5.7
OL two-staged	0	21.0	82	17.7
OL two-staged	5	21.5	87	16.7
OL two-staged	10	22.0	99	14.5
OL two-staged	20	23.1	118	12.3
OL two-staged	30	24.3	117	12.4
OL two-staged	40	25.6	114	12.8
OL two-staged	60	29.0	130	11.2
OL two-staged	80	33.0	149	9.7

Table A2. Error analysis for the heat fluxes.

Test—Combustion Regime	O_2 Flow Rate [Nm^3/h]	Overall O_2 Conc. [%]	Relative error						
			Sec. 1 [%]	Sec. 2 [%]	Sec. 3 [%]	Sec. 4 [%]	Sec. 5 [%]	Sec. 6 [%]	Sec. 7 [%]
PE one-staged	0	21.0	4.7	2.6	1.7	2.0	2.2	2.7	2.0
PE one-staged	20	23.1	3.8	2.2	1.8	1.8	2.1	2.6	2.0
PE one-staged	40	25.6	4.1	2.2	1.5	1.8	2.0	2.4	2.0
PE one-staged	80	33.0	3.0	1.7	1.3	1.6	1.6	2.1	2.0
PE two-staged	0	21.0	3.5	1.6	1.3	1.9	1.9	2.3	2.1
PE two-staged	20	23.1	3.8	1.8	1.5	1.9	2.3	2.7	2.4
PE two-staged	40	25.6	2.9	1.4	1.3	1.7	2.1	2.7	2.6
PE two-staged	80	33.0	2.6	1.3	1.1	1.6	2.1	2.3	2.6
AO one-staged	0	21.0	4.7	2.6	1.7	2.0	2.2	2.7	2.0
AO one-staged	20	23.1	3.7	2.3	1.6	2.0	2.2	2.6	2.2
AO one-staged	40	25.6	4.1	2.1	1.5	1.7	1.9	2.0	1.9
AO one-staged	80	33.0	3.0	1.7	1.4	1.5	1.6	1.7	1.7
AO two-staged	0	21.0	3.5	1.6	1.3	1.9	1.9	2.3	2.1
AO two-staged	20	23.1	3.6	1.8	1.5	1.9	2.2	2.6	2.3
AO two-staged	40	25.6	3.1	1.5	1.4	1.7	2.0	2.1	2.0
AO two-staged	80	33.0	2.5	1.6	1.3	1.6	1.7	2.2	2.0
OL one-staged	0	21.0	4.7	2.6	1.7	2.0	2.2	2.7	2.0
OL one-staged	20	23.1	3.2	1.9	1.5	1.7	2.1	2.7	2.1
OL one-staged	40	25.6	3.6	2.3	1.6	1.7	2.1	2.4	1.8
OL two staged	0	21.0	3.5	1.6	1.3	1.9	1.9	2.3	2.1
OL two-staged	20	23.1	2.4	1.5	1.3	1.8	2.0	2.6	2.0
OL two-staged	40	25.6	2.8	1.8	1.4	1.7	2.1	2.6	2.2
OL two-staged	80	33.0	2.0	1.2	1.2	1.6	2.2	2.9	2.6

References

1. Baukal, C.E. *Industrial Burners Handbook*; CRC Press LLC: Boca Raton, FL, USA, 2004.
2. Baukal, C.E. *Oxygen-Enhanced Combustion*; CRC Press LLC: Boca Raton, FL, USA, 1998.
3. Mondal, M.K.; Balsora, H.K.; Varchney, P. Progress and trends in CO_2 capture/separation technologies: A review. *Energy* **2012**, *46*, 431–441. [CrossRef]
4. Wall, T.F. Combustion processes for carbon capture. *Proc. Combust. Inst.* **2007**, *31*, 31–47. [CrossRef]
5. Gronkvist, S.; Bryngelsson, M.; Westermark, M. Oxygen efficiency with regard to carbon capture. *Energy* **2006**, *31*, 3220–3226. [CrossRef]
6. Li, B.; Duan, Y.; Luebke, D.; Morreale, B. Advances in CO_2 capture technology: A patent review. *Appl. Energy* **2013**, *102*, 1439–1447. [CrossRef]
7. Wu, K.K.; Chang, Y.C.; Chen, C.H.; Chen, Y.D. High-efficiency combustion of natural gas with 21–30% oxygen-enriched air. *Fuel* **2010**, *89*, 2455–2462. [CrossRef]
8. Merlo, N.; Boushaki, T.; Chauveau, C.; Persis, S.D.; Pillier, L.; Sarh, B.; Gökalp, I. Combustion characteristics of methane-oxygen enhanced air turbulent non-premixed swirling flames. *Exp. Therm. Fluid Sci.* **2014**, *56*, 53–60. [CrossRef]
9. Tan, Y.; Douglas, M.A.; Thambimuthu, K.V. CO_2 capture using oxygen enhanced combustion strategies for natural gas power plants. *Fuel* **2002**, *81*, 1007–1016. [CrossRef]
10. Horbaniuc, B.; Marin, O.; Dumitrascu, G.; Charon, O. Oxygen-enriched combustion in supercritical steam boilers. *Energy* **2004**, *29*, 427–448. [CrossRef]
11. Sánchez, M.; Cadavid, F.; Amell, A. Experimental evaluation of a 20 kW oxygen enhanced self-regenerative burner operated in flameless combustion mode. *Appl. Energy* **2013**, *111*, 240–246. [CrossRef]
12. Qiu, K.; Hayden, A.C.S. Increasing the efficiency of radiant burners by using polymer membranes. *Appl. Energy* **2009**, *86*, 349–354. [CrossRef]
13. Lambert, J.; Sorin, M.; Paris, J. Analysis of oxygen-enriched combustion for steam methane reforming (SMR). *Energy* **1997**, *22*, 817–825. [CrossRef]
14. Coombe, H.S.; Nieh, S. Polymer membrane air separation performance for portable oxygen enriched combustion applications. *Energy Convers. Manag.* **2007**, *48*, 1499–1505. [CrossRef]
15. Bělohradský, P.; Skryja, P.; Hudák, I. Experimental study on the influence of oxygen content in the combustion air on the combustion characteristics. *Energy* **2014**, *75*, 116–126. [CrossRef]
16. Kermes, V.; Bělohradský, P. Biodiesel (EN 14213) heating oil substitution potential for petroleum based light heating oil in a 1 MW stationary combustion facility. *Biomass Bioenergy* **2013**, *49*, 10–21. [CrossRef]
17. Baukal, C.E. *Industrial Combustion Pollution and Control*; Marcel Dekker: New York, NY, USA, 2004.
18. Prieler, R.; Bělohradský, P.; Mayr, B.; Rinner, A.; Hochenauer, C. Validation of Turbulence/Chemistry Interaction Models for use in Oxygen Enhanced Combustion. *Energy Procedia* **2017**, *120*, 548–555. [CrossRef]
19. Persis, S.; Foucher, F.; Pillier, L.; Osorio, V.; Gökalp, I. Effects of O_2 enrichment and CO_2 dilution on laminar methane flames. *Energy* **2013**, *55*, 1055–1066. [CrossRef]
20. Abdelaal, M.M.; Rabee, B.A.; Hegab, A.H. Effect of adding oxygen to the intake air on a dual-fuel engine performance, emissions, and knock tendency. *Energy* **2013**, *61*, 612–620. [CrossRef]
21. Souza, G.R.; Santos, A.M.; Ferreira, A.L.; Martins, K.C.R.; Módolo, D.L. Evaluation of the performance of biodiesel from waste vegetable oil in a flame tube furnace. *Appl. Therm. Eng.* **2009**, *29*, 2562–2566. [CrossRef]
22. Bašta, J. *Heat Transfer Surfaces*; ČVUT: Prague, Czech Republic, 2001. (In Czech)
23. Braembussche, V.D. *Measurement Techniques in Fluid Dynamics: An Introduction*; Von Karman Institute for Fluid Dynamics: Rhode Saint Genése, Belgium, 2001.
24. Bevington, P.; Robinson, D.K. *Data Reduction and Error Analysis for the Physical Sciences*; McGraw-Hill: New York, NY, USA, 2002.